10th World Congress on Structural and Multidisciplinary Optimization
May 19 -24, 2013, Orlando, Florida, USA

Smart Sensing Function Design Using Multifunctional Material for Failure Diagnostics and Prognostics

Abdulaziz T. Almaktoom[1], Zequn Wang[2], Pingfeng Wang[3], and Soobum Lee[4]

[1,2,3]Department of Industrial and Manufacturing Engineering, Wichita State University Wichita, KS 67260, USA, atalmaktoom@wichita.edu, zxwang5@wichita.edu, pingfeng.wang@wichita.edu
[4]Department of Mechanical Engineering, University of Maryland, Baltimore County Baltimore, MD 21250, USA, sblee@umbc.edu

1. Abstract
Multifunctional structural materials possess attractive attributes that can be designed to realize smart system functionalities such as integrated sensing systems for failure diagnostics and prognostics. With integrated sensing capabilities enabled by multifunctional structural materials, real-time monitoring of potentially damaging structural responses becomes possible. However, due to various uncertainties introduced by structural material properties, manufacturing processes, as well as operating conditions, ensuring the robustness of sensing performance is of vital importance for smart sensing system development. This paper presents a reliability-based robust design approach to develop piezoelectric materials based structural sensing systems for failure diagnostics and prognostics. In the proposed approach, a detectability measure is defined to evaluate the performance of any given sensing system being designed. With the detectability measure, a sensing system design problem can be transformed to a problem of maximizing detectability values for different failure modes through optimally allocating piezoelectric materials into a target structural system. This transformed problem can be conveniently formulated into a reliability-based robust design framework to ensure design robustness while considering the uncertainties. Two engineering design case studies will be employed to demonstrate the efficacy of the proposed methodology in developing multifunctional material sensing systems.

2. Keywords: Reliability-based robust design, Multifunctional material systems, Failure diagnostics and prognostics, Piezoelectric materials

3. Introduction
With the increasing complexity of engineering system, failure diagnostics and prognostics (FDP) technique is employed to prevent the potential catastrophic failure. This technique has been applied successfully on engineering structures such as automotive industry, turbine, aerospace, and transformers among many others [1]-[7]. This FDP system should be able to monitor structural systems, recognize the state and severity of damages, and also indicate the future structural health state which helps evaluate system's health conditions and the remaining useful lives (RULs).

Multifunctional material for FDP holds advanced characteristics beyond the strength and arduousness that normally ambition research disciplines and engineers. Furthermore, it can be designed to have integrated functionalities to compensate the basic material capabilities. There is no doubt that FDP can impact maintenance strategies and working efficiency. RUL also can be increased by implementing FDP appropriately [8], while FDP can be costly and inefficient unless it is appropriately implemented [9]. Still there is a need to enhance FDP systems by increasing sensing detectability. Multifunctional material sensing system has been studied to improve the detectability and reduce uncertainty that can contaminate measured detectability [10]. In [11], sensor placement design is studied for structural health monitoring under uncertainty. In [12], optimal location of sensors is presented for parametric identification of linear structural systems. A methodology for optimally locating sensors in a dynamic system presented in [13], [14] proposed a probabilistic approach for optimal sensor allocation in structural health monitoring system. [15] Developed a Bayesian approach to optimal sensor placement for structural health monitoring with application to active sensing. In [16], an optimal sensor location methodology for structural identification and damage detection is studied. Most of these methods were settled for allocating a number of sensors to distinguish a specific health state of structural damage, and their applications are limited by the type of health state failure mechanisms.

However, due to various uncertainties introduced by structural material properties, manufacturing processes, as well as operating conditions, ensuring the robustness of sensing performance is a vital importance for smart sensing system development. Reliability based robust design optimization (RBRDO) is developed recently in order to guarantee the desired quality and reliability and minimize uncertainties. RBRDO aims to qualify the

performance of engineered systems by regulating design characteristics and constraints for robustness and reliability by considering cost, variability, and uncertainties involved in the process of system design, operating conditions, manufacturing processes, and structural materials into account. Numerous studies have been developed to deal with uncertainties [17]-[20] and robustness associated with reliability [21]-[26].

To customize RBRDO for sensing system design problem, RBRDO of multifunctional sensing system for FDP is developed in this paper using piezoelectric material. In RBRDO, the detectability of sensing system under uncertainty is defined and the design problem is formulated to minimize the lifecycle cost while satisfying the predefined detectability target. The rest of the paper is organized as follows. First, smart sensing with piezoelectric materials is introduced in section 4. In section 5, a detectability measure is defined in a probabilistic form as a unified quantitative measure for the performance of any given sensing system used for the structural health diagnostics. A general approach for detectability evaluation is also introduced based on health state classification. In section 6, a generic RBRDO framework is developed to design smart material systems for the structural health diagnostics and prognostics. A rectangular plate case study is used in section 7 to demonstrate the efficacy of the proposed methodology in developing multifunctional material sensing systems.

4. Smart Sensing with Piezoelectric Materials

Piezoelectric materials can be potentially applied for real-time monitoring of structural damages, utilizing direct piezoelectric effect – generation of electric potential in response to an applied mechanical stress. One of the commonly used piezoelectric materials is lead zirconate titanate (PZT) [27], a piezoelectric ceramic, which has wide application in vibration sensors and health monitoring systems [28]: a self-sensing piezoelectric actuator for collocated control [29], health monitoring/damage detection of a rotorcraft planetary gear train system using piezoelectric sensors [30], and smart sensor system for structural condition monitoring of wind turbines [31]. In this paper a new smart sensing system design framework will be developed for FDP using piezoelectric materials.

Piezoelectric materials constitutive relationship can be formulated mathematically [32][39] and used in both actuating and sensing applications. In actuating applications the PZT actuator is attached to a structure and an external electric source is applied to the actuator that induce strain field. In sensing applications the PZT sensor is attached to a structure and exposed to a stress field that creates electric charges. In both cases a coupled field problem is solved as follows:

$$\varepsilon_k = d^c_{jk} E_j + s^E_{km} \sigma_m \tag{1}$$

$$D_i = e^\sigma_{ij} E_j + d^d_{im} \sigma_m \tag{2}$$

where, ε is a vector of the strain, d^c_{jk} is a vector of the piezoelectric coefficient that defines strain per unit at constant stress (m/V), E is a vector of the electric field (V/m), s^E_{km} is a vector of the elastic compliance (m2/N), σ_m is a vector of the stress (N/m2). D is a vector of the electric displacement (Coulomb/m2), e^σ_{ij} is a vector of the dielectric permittivity (F/m). This paper considers a sensing application which utilizes d_{31} effect of PZT material: a voltage output along the thickness direction as a response of in-plane strain see Figure 1.

This paper makes use of a harmonic vibration model with a fixed frequency for the design of a piezoelectric energy harvester. Harmonic response analysis solves the time-dependent equation of motion for linear structures under steady-state vibration with a fixed excitation frequency. Considering a general equation of motion for a piezoelectric coupled-field structure after the application of the vibrational principle and finite element (FE) discretization, the coupled FE matrix equation is derived as [25]:

$$\begin{bmatrix} \mathbf{M} & \mathbf{0} \\ \mathbf{0} & \mathbf{0} \end{bmatrix} \begin{Bmatrix} \ddot{u} \\ \ddot{V} \end{Bmatrix} + \begin{bmatrix} \mathbf{D} & \mathbf{0} \\ \mathbf{0} & \mathbf{0} \end{bmatrix} \begin{Bmatrix} \dot{u} \\ \dot{V} \end{Bmatrix} + \begin{bmatrix} \mathbf{K} & \mathbf{K}^z \\ (\mathbf{K}^z)^{\mathrm{T}} & \mathbf{K}^d \end{bmatrix} \begin{Bmatrix} u \\ V \end{Bmatrix} = \begin{Bmatrix} F \\ L \end{Bmatrix}, \tag{3}$$

where M, D, and K are the structural mass, damping, and stiffness matrices respectively, K^z is piezoelectric coupling matrix, K^d is dielectric conductivity matrix, {u} is displacement vector, {V} is voltage vector, and {F} and {L} are structural and electrical load vectors. The electrical load vector is assumed to be zero in this paper, {L} = 0; only the structural input loading exists for the design of energy harvester. In the harmonic response analysis, all points in the structure are vibrating at the same known frequency. Therefore the displacements and voltage may be defined as:

$$\begin{aligned} \{u\} &= \{u_{\max}\} e^{j(\varphi+\omega t)} = \{u_{\max} (\cos\varphi + j \sin\varphi)\} e^{j\omega t} = \left[\{u_{re}\} + j\{u_{im}\}\right] e^{j\omega t} \\ \{V\} &= \{V_{\max}\} e^{j(\varphi+\omega t)} = \{V_{\max} (\cos\varphi + j \sin\varphi)\} e^{j\omega t} = \left[\{V_{re}\} + j\{V_{im}\}\right] e^{j\omega t}, \end{aligned} \tag{4}$$

where $\{u_{max}\}$ and $\{V_{max}\}$ are the maximum displacement (maximum voltage), φ is the phase angle, ω is the

imposed excitation frequency, j is square root of -1, and the sub-indices *re* and *im* represent the real and imaginary components, respectively. The force vector can be specified analogously as follows:

$$\{F\} = \{F_{\max}\} e^{j(\varphi+\omega t)} = \{F_{\max}(\cos\varphi + j\sin\varphi)\} e^{j\omega t} = \left[\{F_{re}\} + j\{F_{im}\}\right] e^{j\omega t} \tag{5}$$

Finally, substituting Eq. (4) and Eq. (5) into Eq. (3) and cancelling $e^{j\omega t}$, we obtain that [39]

$$\left(-\omega^2 \begin{bmatrix} \mathbf{M} & \mathbf{0} \\ \mathbf{0} & \mathbf{0} \end{bmatrix} + j\omega \begin{bmatrix} \mathbf{C} & \mathbf{0} \\ \mathbf{0} & \mathbf{0} \end{bmatrix} + \begin{bmatrix} \mathbf{K} & \mathbf{K}^z \\ (\mathbf{K}^z)^{\mathrm{T}} & \mathbf{K}^d \end{bmatrix}\right) \begin{bmatrix} \{u_{re}\} + j\{u_{im}\} \\ \{V_{re}\} + j\{V_{im}\} \end{bmatrix} = \begin{bmatrix} \{F_{re}\} + j\{F_{im}\} \\ \mathbf{0} \end{bmatrix} \tag{6}$$

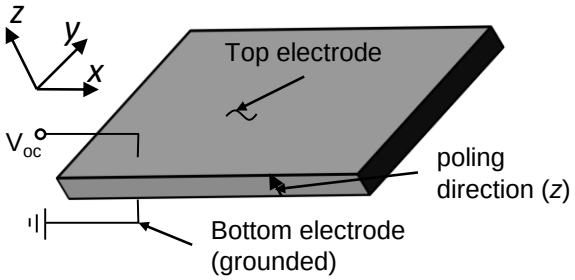

Figure 1: Schematic of a piezoelectric ceramic sheet

5. Probabilistic Detectability Measure and Evaluation

The sensing system can monitor physical behaviors and determine the health state of a system. However, false alarm may occur due to the uncertainties on system operation processes and manufacturing. Therefore, the performance of sensing system should be qualified using a probabilistic method, so that the accurate detection of system health states can be achieved. In the proposed RBRDO of sensing system for FDP framework, a set of health states must be categorized based on historical failure data. Thus correct and incorrect detection rates of every health state will be defined as the sensing performance measures. The correct classification rate of particular health state can be calculated using a conditional probability so that the sensing system can detect the true health state and identify at which state the system is operated. On contrast, the incorrect detection rate can also expressed as a conditional probability that the sensing system detects wrong information. Using the data of correct and incorrect detection rates, the sensing system detectability can be defined by establishing the probability-of-detection (PoD) matrix.

This section introduce the concept of detectability and the method to evaluate the detectability for each health state based on structural simulation and system health state classification. Subsection 5.1 introduces the concept of probability of detection matrix to qualify the sensing system. Subsection 5.2 presents the Mahalanobis distance based approach for health state classification. In this research, it is assumed that all numerical models are valid and they deliver accurate results associated with actual systems.

5.1. Probability-of-detection (PoD) matrix

PoD matrix helps to define the overall sensing system detection performances that represent the probabilities of correct detection for all predefined health states. A general form of the PoD matrix is shown in Table 1.

Table 1: Probability of detection (PoD) matrix

Probability		**Detected Health State**				
		1	2	3	…	N_{HS}
True Health State	1	P_{11}	P_{12}	P_{13}	…	$P_{1N_{HS}}$
	2	P_{21}	P_{22}	P_{23}	…	$P_{2N_{HS}}$
	…	…	…	…	…	…
	N_{HS}	$P_{N_{HS}1}$	$P_{N_{HS}2}$	$P_{N_{HS}3}$	…	$P_{N_{HS}N_{HS}}$

In the PoD matrix N_{HS} represents the number of health states (*HS*), where P_{ij} indicates the probabilistic relationship between the true system health state and the health state detected by the sensing system. P_{ij} can be defined as the conditional probability that the system is detected to be operated at HS_j by the sensing system given that the system is operated at HS_i, where the i^{th} represents a conditional probability of correct detection for the i^{th}

health state. This relation can be statistically expressed as shown in Eq. (7).

$$P_{ij} = Pr\left(Detected\ as\ HS_j \mid System\ is\ at\ HS_i\right) \tag{7}$$

To provide a probabilistic measure for FDP performance of a sensing system while considering uncertainty in manufacturing and system operation processes, it is a must to define the detectability of the i^{th} system health state (HS_i) based on the PoD matrix. The detectability of a *HS* system can be statistically defined, See Eq. (8) below for the demonstration.

$$D_i = P_{ii} = Pr\left(Detected\ as\ HS_i \mid System\ is\ at\ HS_i\right) \tag{8}$$

In this example there is only one sensor will be used for damage detection and three predefined health states as following:

- Health State 1 (HS_1): The system is operating normally without any damage and follows a normal distribution as $N(2, 0.9^2)$
- Health State 2 (HS_2): The system is operating but has some minor damage that follows a normal distribution as $N(3, 0.6^2)$
- Health State 3 (HS_3): The system is operating but has a severe damage that follows a normal distribution as $N(7, 1.5^2)$

Now will measures detectability values for all three defined health states based on the available information. The *z*-score is calculated to define a normalized distance between the testing data and the sensor output distribution for the three predefined health state. This step will classify all given data set of testing sensory into one of the three health states. A normalized distance will classify the collected data from the sensor output distribution of each health state that would categorize the testing data into the health state that has the minimum normalized distance. Boundaries between two health states will be identified by one neutral point that leads to three equal normalized distances as shown in Figure 2.

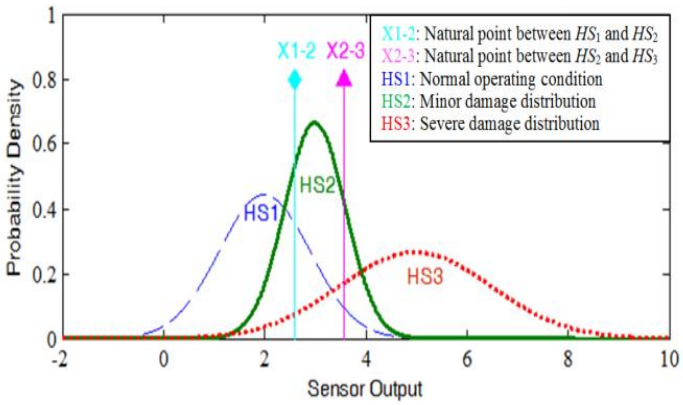

Figure 2: Sensor output distributions neural points

The natural point ($X_{1\text{-}2}$) between HS_1 and HS_2 can be calculated using Eq. (9), and the natural point ($X_{2\text{-}3}$) between HS_2 and HS_3 can be calculated as shown in Eq. (10). Then detectability (D_i) can be evaluated as shown in Eq. (11, 12, and 13) using conditional probability procedure that defined in Eq. (7).

$$\frac{X_{1-2}-2}{0.9} = \frac{3-X_{1-2}}{0.6},\ X_{1-2} = 2.6 \tag{9}$$

$$\frac{X_{2-3}-3}{0.6} = \frac{5-X_{2-3}}{1.5},\ X_{2-3} = 3.57143 \tag{10}$$

$$\begin{aligned} D_1 = P_{11} &= \Pr(\text{Detected as } HS_1 \mid \text{System is at } HS_1) \\ &= \Pr\left(X \le X_{1-2} \mid X \sim N\left(2, 0.9^2\right)\right) \\ &= 0.7475 \end{aligned} \tag{11}$$

$$D_2 = P_{22} = \Pr(\text{Detected as } HS_2 \mid \text{System is at } HS_2)$$
$$= \Pr\left(X_{1-2} \le X \le X_{2-3} \mid X \sim N\left(3, 0.6^2\right)\right) \quad (12)$$
$$= 0.5771$$

$$D_3 = P_{33} = \Pr(\text{Detected as } HS_3 \mid \text{System is at } HS_3)$$
$$= \Pr\left(X \ge X_{2-3} \mid X \sim N\left(7, 1.5^2\right)\right) \quad (13)$$
$$= 0.8295$$

By solving this mathematical example using analytical evaluation of the detectability, it is clear that statistical distributions and health states classification of sensor outputs are critical for FDP sensing system detectability analysis. Nevertheless, in practical engineering applications, a sensing system for FDP contains numerous sensors to deal with more than three health states. Accordingly, the analytical evaluation of sensing systems detectability becomes very difficult to calculate due to the calculation of neutral points between all health states. Also, statistical distributions of sensors' outputs for all health states are not commonly available. As a substitute, the Mahalanobis distance (MD) classifier is employed to characterize the uncertainties of sensor output for each system health state using training data of the sensors' outputs.

5.2. Mahalanobis Distance Based Health State Classification

This section presents a detectability method using Mahalanobis distance (MD) classifier to calculate the detectability value for each health state based on structural simulation and system health state classification. To classify all health stats in complex sensing systems, the MD classifier quantitatively measures the similarity between the sensors' outputs data set and the training data. The MD classifier has the ability to recognize if one set of testing data is related to another predefined set of training data. In other words, MD classifier can categorize which predefined health state is related to the system health state represented by the testing data. See Eq. (14) below for the demonstration.

$$MD_i = \left(X - M_i\right)^T \Sigma^{-1} \left(X - M_i\right) \quad (14)$$

where the superfix T denotes matrix transpose, and Σ denotes the common covariance matrix of the training data set for his, X is the given testing sensory data set to be classified, and M_i is the vector of mean values of the training data set for the health state HS_i.

One example is used to show the MD based health state classification approach. In this example, there are two sensors used for damage detection and three predefined health states as shown in Table 2. Also, there are five sets of testing data shown in the first two columns in Table 3.

Table 2: Predefined system health states

Health State (HS)	Sensor 1	Sensor 2
HS_1 (Healthy state)	σ*rand(1,n) − 1.4	σ *rand(1,n)
HS_2 (Minor damage)	σ*rand(1,n) − 3	σ *rand (1,n) + 0.7
HS_3 (Severe damage)	σ*rand(1,n)	σ *rand (1,n) − 0.5

Now we will find out the detectability values for all three predefined health states. The MD classifier method is used to define a normalized distance between the testing data and the sensor output distribution for the three predefined health states. This step will classify each testing data set into a specific health state with the smallest MD value.

Table 3: System Health States Classification Using MD Classifier

Sensory Data		Mahalanobis Distance			Classified State
S_1	S_2	HS_1	HS_2	HS_3	
-1.66	0.13	14.40	69.50	163.50	HS_1
-2.26	0.89	269.56	12.15	418.32	HS_2
-0.96	0.95	102.02	247.74	221.35	HS_1
-2.48	-0.31	84.74	90.99	264.06	HS_1
0.09	-1.64	999.68	563.43	172.23	HS_3

Table 3 demonstrates system health states classification using MD classifier. The MD values for each testing data set are calculated using Eq. (14). The last column in Table 3 indicates the classified system health states for each sensory data set. PoD matrix can be evaluated based on the MD Classifier as follows. Suppose that there are 75 sets of testing sensory data, and T_{ij} sets classified as exposed in Eq. (15). The probability of detection P_{ij} can be intended based on the PoD matrix, as shown in Eq. (16), then the detectability of the three health stats is calculated using Eq. (17).

$$T_{ij} = \begin{pmatrix} 70 & 3 & 2 \\ 5 & 70 & 0 \\ 32 & 0 & 43 \end{pmatrix} \tag{15}$$

$$P_{ij} \approx \frac{T_{ij}}{\sum_j T_{ij}} = \begin{pmatrix} 0.93 & 0.04 & 0.03 \\ 0.07 & 0.93 & 0 \\ 0.43 & 0 & 0.57 \end{pmatrix} \tag{16}$$

$$D_i = P_{ii} \approx \begin{pmatrix} 0.93 & 0.93 & 0.57 \end{pmatrix} \tag{17}$$

6. Reliability Based Robust Design Optimization Formulation

RBRDO aims to find the best compromise between cost and reliability by taking uncertainties into account. Moreover, it is used to control reliability and reduce cost variances by minimizing cost and its uncertainty factors (variance) while meeting the required reliability and detectability. To tackle detectability issues, the design of a multifunctional sensing system for FDP is formulated with RBRDO to maximize the detectability for different failure modes by optimally allocating PZT sensor. The PZT sensor network can be demonstrated by Figure 3.

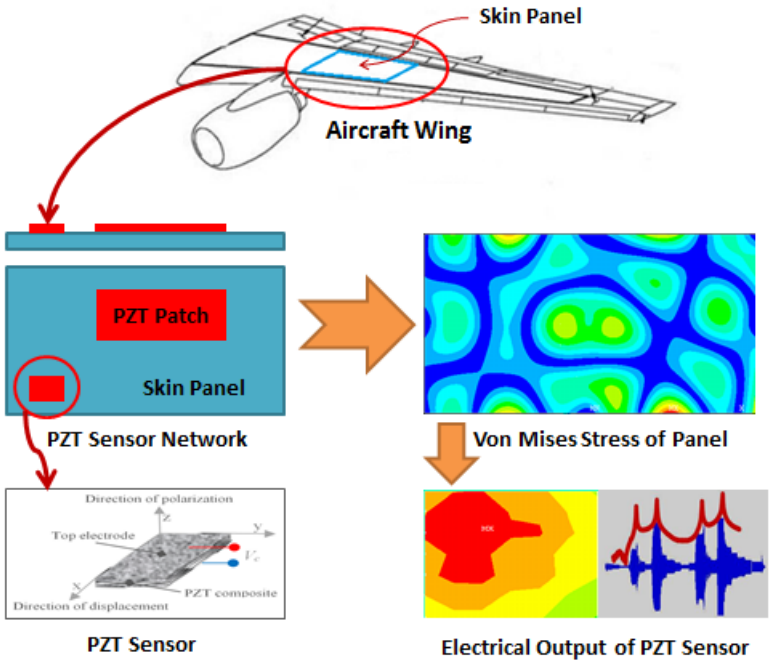

Figure 3: Reliability-based Robust Design of Sensor Network

In this study, RBRDO of PZT sensing system for FDP can be formulated as a multi objective optimization problem as follows:

$$
\begin{aligned}
&\textit{Minimize} \quad \sum_{j=1}^{nf} M_f(X;d) + Q_f(H(X;d)) \\
&\textit{subject to :} \\
&\qquad prob(G_i(X,d) \le 0) \beta_{t_i}) \\
&\qquad prob(D_i(X,d) \ge \beta_{D_i}), \qquad i = 1,....,n \\
&\qquad x^L \le x \le x^U, \quad X \in R^{nr} \\
&\qquad d^L \le d \le d^U, \quad d \in R^{nd}
\end{aligned} \tag{18}
$$

where The design constraints involved in the sensing systems design framework are detectability requirements considering uncertainties introduced by PZT material properties, manufacturing processes, as well as operating conditions. The design variables are the decision variables for PZT sensors dimension, PZT sensors locations, and the parameters for controlling the sensing process. As the intent of the sensing systems design optimization is to minimize the cost while satisfying the detectability requirements. The cost can be determined by knowing sensors size.

The objective is to minimize PZT sensor size and its variance. Where, $M(X;d)$ is the cost on PZT material design, sensing system design, and installation, Q_c ($H(X;d)$) is the quality loss cost (variation associated with the PZT sensor size), G_i is the probabilistic performance function, β_t is the reliability target, D_i is the detectability of the sensing system for the HS_i, β_{Di} is the target detectability for the HS_i, x^U and x^L are upper and lower random design variables X. d^U and d^L are upper and lower deterministic design variables d, and n, n_r ,and n_f, are the numbers of probabilistic constraints, random variables, design variables, and objective functions.

7. Design Case Study

This section demonstrates the proposed RBRDO approach by designing PZT material for FDP of a rectangular panel. As shown in Figure 4, the panel has 2 m length and 1 m width and been fastened by eight joints (L1~L8); there is a harmonic force F with 120 HZ on the middle of panel. In this case study, eight health states are considered as shown in Table 4. To identify the healthy state of the panel, four square PZT sensors are attached to the surface of panel. The electrical potential signal, obtained out of the PZT sensors, is used to identify the health state based on the MD classifier.

Table 4: Health States of Panel

Health States	Definition
HS_0	*Healthy state*
HS_1	*Loosening of the joint L6*
HS_2	*Loosening of the joint L7*
HS_3	*Loosening of the joint L4*
HS_4	*Loosening of the joint L6,L7*
HS_5	*Loosening of the joint L6,L4*
HS_6	*Loosening of the joint L4,L7*
HS_7	*Loosening of the joint L4,L6,L7*

The objective function of this RBRDO for FDP is to minimize PZT sensor size and its variance while the detectability of each health state meets its requirement to be greater than the target 0.99. For each sensor, the coordinate and side length of each squared PZT sensor are chosen as design variables, thus totally there are 12 design variables for this case study. All the design variables are assumed to be normal distributed and their upper and lower bounds of means and standard deviation are shown in Table 5. Besides the random design variables, other random parameters are also taken into consideration and listed in Table 6.

Table 5: Design Variables

Variables	Definition	LB	UB	Distribution Type	SD
X_1	*X coordinate of the first sensor*	*0*	*2*	*Normal*	*0.05*
Y_1	*Y coordinate of the first sensor*	*0*	*1*	*Normal*	*0.05*
S_1	*Side length of the first sensor*	*0*	*0.1*	*Normal*	*5e-3*
X_2	*X coordinate of the second sensor*	*0*	*2*	*Normal*	*0.05*
Y_2	*Y coordinate of the second sensor*	*0*	*1*	*Normal*	*0.05*
S_2	*Side length of the second sensor*	*0*	*0.1*	*Normal*	*5e--3*
X_3	*X coordinate of the third sensor*	*0*	*2*	*Normal*	*0.05*
Y_3	*Y coordinate of the third sensor*	*0*	*1*	*Normal*	*0.05*
S_3	*Side length of the third sensor*	*0*	*0.1*	*Normal*	*5e-3*
X_4	*X coordinate of the fourth sensor*	*0*	*2*	*Normal*	*0.05*
Y_4	*Y coordinate of the fourth sensor*	*0*	*1*	*Normal*	*0.05*
S_4	*Side length of the fourth sensor*	*0*	*0.1*	*Normal*	*5e--3*

Table 6: Random Parameters

Parameters	Definition	Distribution Type	Mean	Standard Deviation
L	*Length of Panel*	*Normal*	*2*	*0.1*
W	*Width of Panel*	*Normal*	*1*	*0.05*
F	*Amplitude of Force*	*Normal*	*1000*	*50*

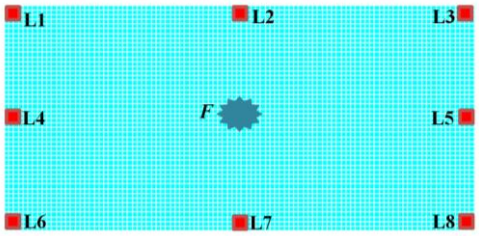

Figure 4: Rectangular plate with indicated damages

To get the electrical potential response of PZT attached on the panel, a 3D finite element model is established in ANSYS 12. Figure 5 shows a particular sensor layout and its vibration displacement of health states HS_0.

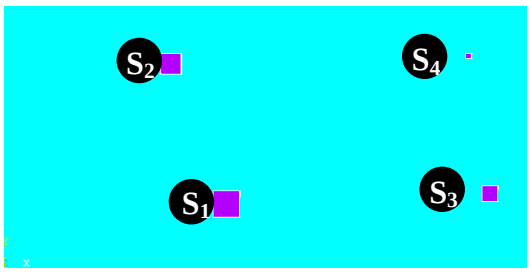

a) Sensor Locations and Designed PZT Geomtry

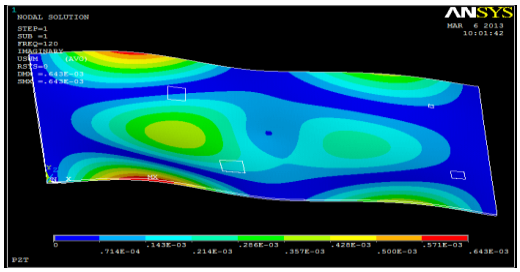

b) Vibration displacement of HS_0

Figure 5: Sensor Layout and Vibration Displacement Contour of the Panel

The location and size of PZT sensor can directly determine the electrical potential response given a certain scenario. In this case, sensor S_1 and S_2 get relative significant electrical response while there is almost no obvious electrical potential for sensor S_3 and S_4. The average electrical potential of each PZT layer is extracted as signal output. Due to the uncertainties involved from not only the whole structural but also the sensing system, the signal output of each sensor is also a random value. Figure 6 demonstrates the distribution of signal outputs given all the uncertainties listed in Table 6 and 7.

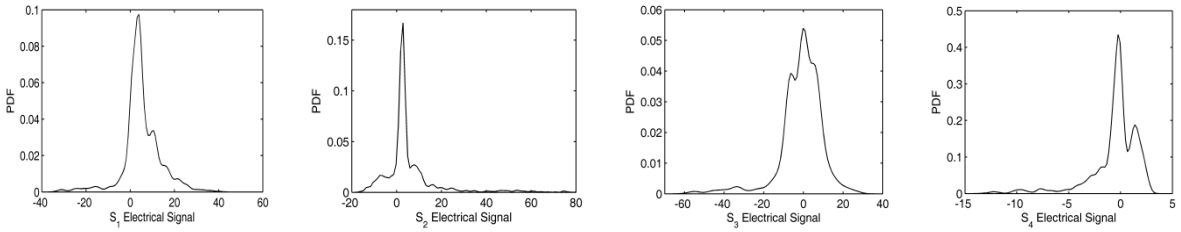

a) S_1 Sensor b) S_2 Sensor c) S_3 Sensor d) S_4 Sensor

Figure 6: The Distribution of Signal Outputs

Generic algorithm is used to search optimal solution for the RBRDO problem, and the optimal design is obtained after 15 generations. The design history is shown in Table 7 while the corresponding detectability and cost are shown in Table 8 in which C_T represents the total cost comprising design cost M and quality lost Q_c. The corresponding detectability of each generation is also shown in Figure 7. Figure 8 demonstrates the cost distribution of initial and optimum design while Figure 9 shows the costs of iterations during RBRD process. As shown in the Figure 8; both the mean and variance of design cost are increased slightly while the detectability of sensing system is improved significantly.

Table 7: Design History during RBRD

Iter.	X_1 (cm)	Y_1 (cm)	S_1 (cm)	X_2 (cm)	Y_2 (cm)	S_2 (cm)	X_3 (cm)	Y_3 (cm)	S_3 (cm)	X_4 (cm)	Y_4 (cm)	S_4 (cm)
1	12.00	12.00	3.00	110.00	60.00	3.00	12.00	60.00	3.00	110.00	60.00	3.00
2	23.64	17.87	3.80	175.64	71.10	3.20	18.52	65.55	6.79	175.70	61.45	5.77
3	71.91	27.42	5.11	115.07	71.65	3.44	68.83	64.02	6.07	139.60	67.59	3.03
4	71.91	25.34	3.45	115.07	77.63	3.44	68.83	64.02	6.07	168.58	69.27	3.03
5	71.91	25.34	3.45	115.07	77.63	3.44	68.83	64.02	6.07	139.60	69.27	3.03
6	73.91	25.34	3.45	115.07	77.63	3.44	68.83	64.02	4.07	141.60	69.27	3.03
7	75.91	25.34	3.45	115.07	77.63	3.44	68.83	64.02	4.07	141.60	69.27	3.03
8	75.91	25.34	3.45	167.15	77.63	3.00	68.83	60.31	4.07	141.60	69.27	3.03
9	75.91	25.34	3.45	167.15	77.63	3.00	68.83	60.31	4.07	141.60	69.27	3.03
10	73.91	25.34	3.45	115.07	77.63	3.00	68.83	60.31	4.07	141.60	69.27	3.03
11	73.91	25.34	3.45	115.07	77.63	3.00	68.83	60.31	4.07	142.60	69.27	3.03
12	76.91	25.34	3.45	115.07	79.35	3.00	68.83	60.31	3.07	142.60	69.27	3.03
13	76.91	25.34	3.45	115.07	79.35	3.00	68.83	60.31	3.07	142.60	69.27	3.03
14	76.91	25.34	3.45	115.07	79.35	3.00	68.83	60.31	3.07	142.60	69.27	3.03
15	76.91	25.34	3.45	115.07	79.35	3.00	68.83	60.31	3.07	142.60	69.27	3.03

Table 8: Detectability and cost during RBRD

Iter.	D_0	D_1	D_2	D_3	D_4	D_5	D_6	D_7	M	Q_c	C_T
1	0.79	0.96	0.93	0.95	0.90	0.97	0.94	0.95	36.00	5.76	41.76
2	0.96	1.00	0.98	0.98	1.00	1.00	0.99	1.00	104.04	16.72	120.76
3	0.97	0.99	0.97	0.99	1.00	1.00	1.00	0.99	84.00	13.45	97.45
4	0.98	0.98	1.00	0.99	0.99	1.00	1.00	0.98	69.76	11.10	80.86
5	0.99	1.00	1.00	1.00	1.00	1.00	1.00	0.99	69.76	11.21	80.97
6	0.99	1.00	1.00	1.00	1.00	1.00	1.00	0.99	49.48	7.91	57.39
7	0.99	1.00	1.00	1.00	1.00	1.00	1.00	0.99	49.48	7.93	57.41
8	0.98	0.99	1.00	0.99	1.00	1.00	1.00	1.00	46.62	7.47	54.09
9	0.98	0.99	1.00	0.99	1.00	1.00	1.00	1.00	46.62	7.49	54.11
10	0.98	0.99	1.00	0.99	1.00	1.00	1.00	0.99	46.62	7.44	54.06
11	0.98	0.99	1.00	0.99	1.00	1.00	1.00	0.99	46.62	7.50	54.12
12	0.99	0.99	1.00	1.00	1.00	0.99	1.00	1.00	39.48	6.35	45.83
13	0.99	0.99	1.00	1.00	1.00	0.99	1.00	1.00	39.48	6.31	45.79
14	0.99	0.99	1.00	1.00	1.00	0.99	1.00	1.00	39.48	6.29	45.77
15	0.99	0.99	1.00	1.00	1.00	0.99	1.00	1.00	39.48	6.33	45.81

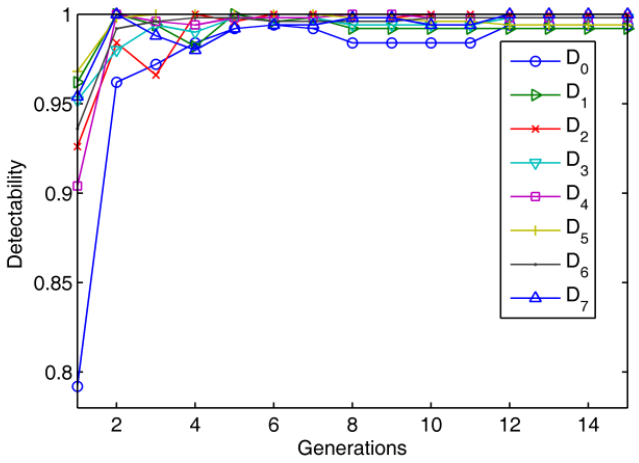

Figure 7: The Detectability during RBRD

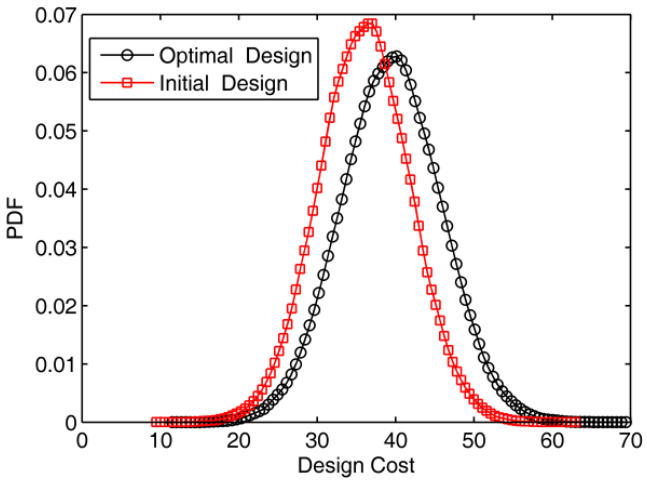

Figure 8: The Cost Distributions of Initial and Optimal Design

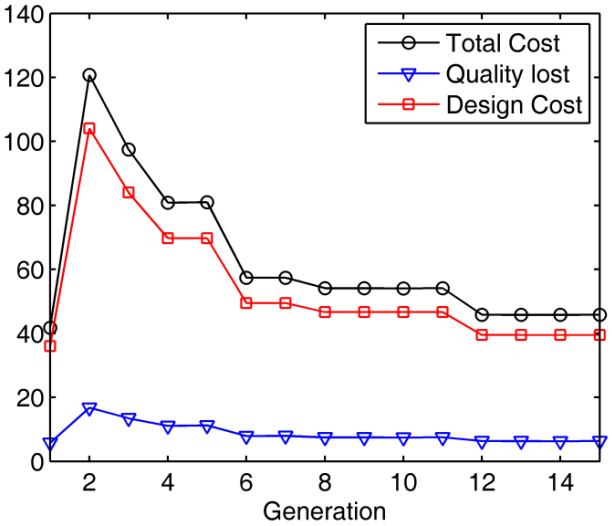

Figure 9: Costs of PZT Design during RBRD process

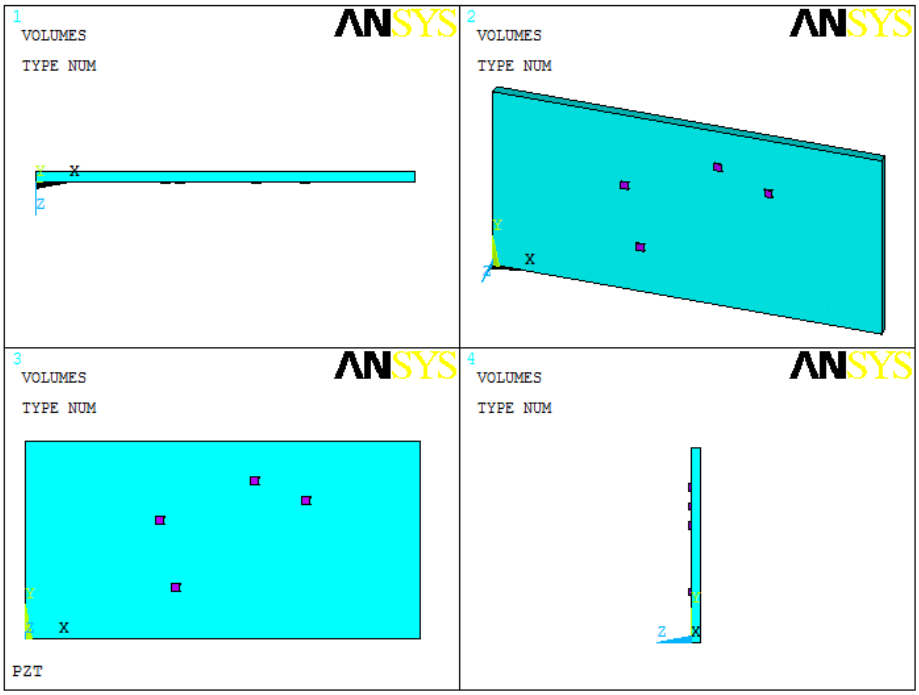

Figure 10: Optimal Sensor Network

8. Conclusion

This paper presented a RBRDO approach to develop piezoelectric materials sensing systems for failure diagnostics and prognostics. In the proposed approach, a multifunctional material sensing systems is defined and used for real-time monitoring of potentially damaging structural responses. The detectability measure is defined to evaluate the performance of a given PZT sensing system. Then, detectability analysis of each health state was developed using MD classifier. Finally, the PZT sensing system design problem is transformed into a problem of maximizing detectability values for different failure modes by optimally allocating PZT sensors and their sizes on a vibrating structure to be monitored. This transformed problem is formulated into a RBRDO framework to ensure design robustness while considering the uncertainties. The rectangular plate case study demonstrated that the proposed RBRDO of PZT sensing system for failure diagnostics and prognostics is feasible to detect different health states in multifunctional material sensing systems under various uncertainties.

9. References

[1] X. Zhao, T. Qian, G. Mei, C. Kwan, R. Zane, C. Walsh, T. Paing, and Z. Popovic, Active health monitoring of an aircraft wing with an embedded piezoelectric sensor/actuator network: II. Wireless approaches, *Smart Materials and Structures*, 16 (4), 1218, 2007.

[2] L. Qing, T. Zhi, Y. Yuejun, and L. Yue, Localized Structural Health Monitoring Using Energy-Efficient Wireless Sensor Networks, *Sensors Journal, IEEE*, 9 (11) 1596-1604, 2009.

[3] N. A. Tanner, J. R. Wait, C. R. Farrar, and H. Sohn, Structural health monitoring using modular wireless sensors," *Journal of Intelligent Material Systems and Structures*, 14 (1), 43-56, 2003.

[4] K. M. Janasak, and R. R. Beshear, Diagnostics To Prognostics - A Product Availability Technology Evolution, Proc. *Reliability and Maintainability Symposium*, 113-118, 2007.

[5] H.-N. Li, D.-S. Li, and G.-B. Song, Recent applications of fiber optic sensors to health monitoring in civil engineering, *Engineering Structures*, 26 (11), 1647-1657, 2004.

[6] E. I. C. M Bocca, J Salminen and L. M Eriksson, A reconfigurable wireless sensor network for structural health monitoring, *presented at the The 4th International Conference on Structural Health Monitoring of Intelligent Infrastructure (SHMII-4)*, Zurich, Switzerland, 2009.

[7] I. E. Alguindigue, A. Loskiewicz-Buczak, and R. E. Uhrig, Monitoring and diagnosis of rolling element bearings using artificial neural networks, *Industrial Electronics, IEEE Transactions on*, 40, 209-217, 1993.

[8] D. Liu, Y. Peng, and X. Peng, Online adaptive status prediction strategy for data-driven fault prognostics of

complex systems, in *Prognostics and System Health Management Conference (PHM-Shenzhen)*, 2011.
[9] F. K. Chang and J. F. C. Markmiller, *A new look in design of intelligent structures with SHM*. Lancaster: Destech Publications, Inc, 2006.
[10] R. V. Field and M. Grigoriu, Optimal design of sensor networks for vehicle detection, classification, and monitoring, *Probabilistic engineering mechanics.*, 21, 305-316, 2006.
[11] R. F. Guratzsch and S. Mahadevan, Sensor placement design for SHM under uncertainty, in *Proc. 3rd European Workshop: Structural Health Monitoring*, 1168-75, 2006.
[12] P. Kirkegaard and R. Brincker, On the optimal location of sensors for parametric identification of linear structural systems, *Mechanical Systems and Signal Processing*, 8, 639-647, 1994.
[13] F. Udwadia, Methodology for Optimum Sensor Locations for Parameter Identification in Dynamic Systems, *Journal of Engineering Mechanics*, 120, 368-390, 1994.
[14] M. Azarbayejani, A. I. El-Osery, K. K. Choi, and M. M. R. Taha, "A probabilistic approach for optimal sensor allocation in structural health monitoring," *SMART MATERIALS AND STRUCTURES*, 17, 055019, 2008.
[15] E. B. Flynn and M. D. Todd, A Bayesian approach to optimal sensor placement for structural health monitoring with application to active sensing, *Mechanical Systems and Signal Processing*, 24, 891-903, 2010.
[16] E. Ntotsios, K. Christodoulou, and C. Papadimitriou, Optimal sensor location methodology for structural identification and damage detection, 2006.
[17] P. Wang, C. Hu, and B. D. Youn, A Generalized Complementary Intersection Method (GCIM) for System Reliability Analysis," *Journal of mechanical design*, 133, 071003, 2011.
[18] Y. Noh, K. K. Choi, I. Lee, D. Gorsich, and D. Lamb, Reliability-Based Design Optimization With Confidence Level for Non-Gaussian Distributions Using Bootstrap Method, *Journal of mechanical design*, 133, 091001, 2011.
[19] B. D. Youn, K. K. Choi, and L. Du, Enriched Performance Measure Approach for Reliability-Based Design Optimization, *AIAA Journal*, 43, 874-884, 2005.
[20] X. Du and W. Chen, Sequential Optimization and Reliability Assessment Method for Efficient Probabilistic Design, *Journal of mechanical design*, 126, 225-233, 2004.
[21] Y. Byeng, W. Pingfeng, and X. Zhimin, Complementary Interaction Method (CIM) for System Reliability Analysis, in *48th AIAA/ASME/ASCE/AHS/ASC Structures, Structural Dynamics, and Materials Conference*, ed: American Institute of Aeronautics and Astronautics, 2007.
[22] Y. Tang, J. Chen, and J. Wei, A sequential algorithm for reliability-based robust design optimization under epistemic uncertainty, *Journal of Mechanical Design*,134, 014502, 2012.
[23] O. P. Yadav, S. S. Bhamare, and A. Rathore, Reliability-based robust design optimization: A multi-objective framework using hybrid quality loss function, *Quality and Reliability Engineering International*, 26, 27-41, 2010.
[24] B. D. Youn, K. K. Choi, and K. Yi, Performance moment integration (PMI) method for quality assessment in reliability-based robust design optimization, *Mechanics Based Design of Structures and Machines*,33, 185-213, 2005.
[25] X. D. He and J. P. Chu, Reliability-Based Robust Design for Mechanical Components under Small-Sample Information, *Applied Mechanics and Materials*, 215, 804-807, 2012.
[26] X. Zhuang, R. Pan, and L. Wang, Robustness and reliability consideration in product design optimization under uncertainty, in *Industrial Engineering and Engineering Management (IEEM), 2011 IEEE International Conference on*, 1325-1329, 2011.
[27] I. S. Rajay Vedaraj, B. V. A. Rao, and B. V. A. Rao, Material analysis for artificial muscle and touch sensing of cooperative biomimetic manipulators, *International Journal of Advanced Manufacturing Technology*, 60, 5-8, 2012.
[28] I. Chopra, Review of current status of smart structures and integrated systems, 20-62, 1996.
[29] J. J. Dosch, D. J. Inman, and E. Garcia, A self-sensing piezoelectric actuator for collocated control, *SPIE milestone series*, 167, 319-338, 2001.
[30] P. Samuel and D. Pines, Health monitoring/damage detection of a rotorcraft planetary geartrain system using piezoelectric sensors, *PROCEEDINGS- SPIE THE INTERNATIONAL SOCIETY FOR OPTICAL ENGINEERING*, 44-55, 1997.
[31] M. J. Schulz, M. J. Sundaresan, L. National Renewable Energy, E. United States. Dept. of, S. United States. Dept. of Energy. Office of, and I. Technical, *Smart Sensor System for Structural Condition Monitoring of*

Wind Turbine, 2006.
[32] J. Sirohi and I. Chopra, Fundamental Understanding of Piezoelectric Strain Sensors, *Journal of Intelligent Material Systems and Structures*,11, 246-257, 2000.
[33] K. Jaehwan, V. V. Vasundara, K. V. Vijay, and B. Xiao-Qi, Finite-element modeling of a smart cantilever plate and comparison with experiments, *Smart Materials and Structures*, 5, 165-170, 1996.
[34] V. Piefort and A. Preumont, Finite element modeling of piezoelectric structures, in *Samtech User's Conference*, 2001.
[35] A. Erturk and D. J. Inman, Appendix A: Piezoelectric Constitutive Equations, in *Piezoelectric Energy Harvesting*, ed: John Wiley & Sons, Ltd, 343-348, 2011.
[36] I. American National Standards, F. Ieee Ultrasonics, C. Frequency Control Society. Standards, E. Institute of, and E. Electronics, *IEEE standard on piezoelectricity*, 1988.
[37] Q. M. Zhang and Z. Jianzhong, Electromechanical properties of lead zirconate titanate piezoceramics under the influence of mechanical stresses, *Ultrasonics, Ferroelectrics and Frequency Control, IEEE Transactions on*, 46, 1518-1526, 1999.
[38] A. M. Sadri, J. R. Wright, and R. J. Wynne, Modelling and optimal placement of piezoelectric actuators in isotropic plates using genetic algorithms, *Smart Materials and Structures*, 8, 490-498, 1999.
[39] S. Lee and A. Tovar, "Topology Optimization of Energy Harvesting Skin Using Hybrid Cellular Automata," J. Mech. Design, 135 (3), 031001, 2013.